Autophagic and phytochemical aspects of color changes in white petals of snapdragon flower during development and senescence

Roghayeh Nabipour Sanjbod[1] · Esmaeil Chamani[1] 🄳 · Younes Pourbeyrami Hir[1] · Asghar Estaji[1]

Abstract

Color change in petals is a clever strategy to attract more pollinators and one of the attractive features of edible flowers for consumers. Several physiological, phytochemical, and ultrastructural factors are involved in this process. However, this phenomenon is well underexplored in white petals. In this study, we investigated the color changes of the white petals of the snapdragon (*Antirrhinum majus* 'Legend White') flower from different aspects during development and senescence. In the ultrastructural analysis, both epidermal and mesophyll cells were examined. During flower development, plastid transition and autophagy processes led to the fading of the green color of young petals and the reduction of starch content, chlorophyll, and carotenoids. The piecemeal chlorophagy was observed in the degradation of starch granules. Leucoplasts were converted into autophagosome-like structures and then disappeared. The presence of these structures was evidence of the transformation of the plastid to the vacuole. As the green color faded, phytochemical compounds were synthesized. With partial flower opening and progression of senescence, pH and phenolic compounds were responsible for color changes. The highest amount of phenolic compound was observed after the flower opening stages. However, Phenolic colored compounds or total anthocyanins became colorless under the influence of low pH. The decrease in starch content caused an increase in the lightness parameter, and the petal color changed to pale yellow.

Introduction

Snapdragon (*Antirrhinum majus* L.) is a spike-type cut flower with various colors and fragrances (Rabiza-Świder et al. 2020). The snapdragon has been considered as a model plant for genetic studies and flower development due to its unique characteristics and a popular plant edible flower due to the presence of some phenolic compounds with high antioxidant properties, attractive taste, scent, and color (González-Barrio et al. 2018; Lian et al. 2020).

The petal color of edible flowers is attractive to consumers and depends on pigment type and distribution (Zhao and Tao 2015; González-Barrio et al. 2018). Flower pigments include four groups: chlorophylls, carotenoids, flavonoids, and betalains (Narbona et al. 2021). The green color of young petals and green tissues is related to chlorophyll in chloroplasts (Zheng et al. 2022). Carotenoids are found in chromoplasts and produce a wide range of yellow, orange, and red colors (Choi et al. 2021). Flavonoids, especially anthocyanins, generate the most diverse colors in flowers and accumulate in vacuoles (Narbona et al. 2021). Flavonoid compounds are responsible for antioxidant properties as well as color and taste (Chamani et al. 2020). Based on plant species, pigments are distributed in epidermal or mesophyll cells (Qi et al. 2013).

Color changes occur in two stages during development: In the cell division stage, the young petals of most flowers contain chlorophyll. With cell expansion, petal pigmentation occurs, in which the chlorophyll content decreases and

✉ Esmaeil Chamani
   echamani@uma.ac.ir

   Roghayeh Nabipour Sanjbod
   rnabipour@uma.ac.ir

   Younes Pourbeyrami Hir
   younes_ph62@uma.ac.ir

   Asghar Estaji
   aestaji@yahoo.com

1 Department of Horticultural Sciences, Faculty of Agriculture and Natural Resources, University of Mohaghegh Ardabili, Ardabil, Iran

🄳 Springer

new pigments are synthesized (Yeon and Kim 2020). Flavonoids have a significant role in petal pigmentation (Deng et al. 2019). In colored petals, anthocyanins often emerge, while in white petals, colorless flavonoid compounds accumulate, such as flavone, flavonol, and flavanone (Zhao and Tao 2015). After flower development and pollination, petals are rapidly senesced. This event is the final stage of petal development and is synonymous with programmed cell death (PCD) (Van Doorn and Woltering 2008; Battelli et al. 2011; Sun et al. 2021).

Color change is one of the visible signs of senescence that may precede wilting (Woltering and Van Doorn 1988). Depending on species, color changes during senescence include the increase of pigments and their fading, affected by pollination, vacuolar pH, and phenolic compounds (Teppabut et al. 2018; Deng et al. 2019; Yeon and Kim 2020; Kanani et al. 2021a). During the senescence of colored petals of *Cymbidium* and *Oenothera laciniata*, anthocyanins are synthesized (Woltering and Van Doorn 1988; Teppabut et al. 2018). In rose flowers, increased flavonoids and anthocyanins have caused petal blueing (Schmitzer et al. 2010). In addition, fading of petal color has been reported in *Nelumbo nucifera* (Liu et al. 2022). Although color changes are pretty evident in colored petals, there is not much information about white petals.

During flower development and senescence, some physiological, phytochemical, and cellular changes happen along with morphological changes. The studies have indicated that as the petals develop, the content of pigment, carbohydrate, phenolic, and pH of cells change (Zhao et al. 2018; Chamani et al. 2020; Kanani et al. 2021b, a). At the subcellular level, plastids undergo plastid transition and become different colored plastids (chromoplasts) in colored petals and colorless plastids (leucoplasts) in white petals. Plastid transition depends on tissue and species type and has been investigated in *Arabidopsis* white petals (Sadali et al. 2019; Choi et al. 2021; Zheng et al. 2022). Plastids may remain until the last stage of senescence or may be degraded during development (Nabipour Sanjbod et al. 2022). However, the plastids' transition and degradation have not been well studied morphologically in white petals.

Autophagy event is activated for the complete degradation of cell components or response to the cell's metabolic demands (Mondal et al. 2021). Cell organelles may be degraded through autophagy pathways and the formation of autophagic structures, as indicated in many studies (Van Doorn et al. 2015; Nabipour Sanjbod et al. 2022; Mizushima 2022). However, the process of organelles degradation has received less attention. TEM (transmission electron microscopy) is the most accurate and reliable method to evaluate the formation of autophagic structures and confirm the results of other autophagy detection analyses in the studied systems (Martí-clua 2022).

Although many plants have white flowers, color change studies have often focused on colored petals and have been less studied on white petals. Furthermore, the morphological, physiological, phytochemical, and cellular characteristics of color changes depend on plant species and have not been understood in the snapdragon. In a previous study, we clearly defined the morphological events of vacuolar cell death and the role of autophagy in the snapdragon (Nabipour Sanjbod et al. 2022). This study investigates underlying events of color changes in the white petals of the snapdragon. The present study provides information about the possible involvement of autophagy and phenolic compounds in color changes. For this purpose, epidermal and mesophyll cells were studied. This study is the first complete description of the color changes in white petals of snapdragon flowers from development to corolla death.

Material and methods

Plant materials, growth conditions and sampling

This experiment was conducted at an experimental greenhouse, the Department of Horticulture, University of Mohaghegh Ardabili, in 2019–2020. Snapdragon F1 (*Antirrhinum majus* 'Legend White') seeds were purchased from Takii Seed Company and germinated at 20 °C under white LED light (light intensity: 3000 lx). The seedlings were cultivated in plastic pots (containing a soil mixture of vermicompost and complete organic fertilizers with a ratio of 3:1) after germination in December. Greenhouse growth conditions included temperatures of 15 to 18 °C, natural daylight, and irrigation every two days. Before flowering, potted plants were transferred to a growth chamber (temperature: 20 °C, RH: 60%, day/night cycle: 16/8 h). We considered eight sampling stages for the longevity of snapdragons, as described in Table 1. At each stage, the first floret was harvested, the upper margins of the dorsal petals were cut into squares (1×1 cm), and flush-frozen with liquid nitrogen. The samples were stored at -80ºC for subsequent measurements.

Fresh and dry weight measurement

Changes in fresh (g) and dry weight (mg) were measured with a digital Micro Balance (Semi-Micro Analytical Balances GR-200, A&D Company, JAPAN). Five corollas were harvested from the first floret of any spike at each time point and weighed immediately to determine the fresh weight. Then, samples were dried in an oven at 80 °C for 48 h and measured for dry weight.

Table 1 Development and senescence stages of snapdragon (*Antirrhinum majus* 'Legend White')

Stage	Description of the floral features
S1 (9 day before flower opening)	The petals were green and entirely covered by sepals (Tight green bud)
S2 (6 day before flower opening)	The green petals emerged out of the sepals (Emerging bud)
S3 (3 day before flower opening)	The petals twist was loosening (Full bud)
S4 (Flower opening)	The flowers were half-open (Half-opened flowers)
S5 (3 day after flower opening)	The petals and anthers are fully opened (Fully opened flower)
S6 (6 day after flower opening)	Partial wilting occurred at the margins of the petals (Wilted flower)
S7 (9 day after flower opening)	The petals wilted severely (Collapsed flower)
S8 (12 day after flower opening)	The petals desiccated (Desiccated flower)

Electrolyte leakage assay

Squares (1×1 cm) were prepared from the margin of the dorsal petal and washed three times with distilled water. The pieces were placed in a glass tube (containing 10 ml of deionized water). Then the glass tubes were placed in a water bath of 25 °C and incubated for 30 min. Initial conductivity was measured with a conductivity meter (WTW InoLab Cond 720 Conductivity Meter, Carl Stuart Limited Company, UK). After that, the glass tubes were placed into a water bath of 96 °C and boiled for 15 min. Subsequently, the glass tubes cooled down to room temperature and were measured for total conductivity. Electrolyte leakage was expressed as the percentage of the initial conductivity versus the total conductivity.

Petal pH measurement

The cell sap pH (vacuolar pH) was determined by grinding 1 g of petals in 10 ml distilled water and occasional stirring. After two hours, petal juice pH was measured by a pH meter (pH-Meter 20 +, CRISON, SPAIN).

Petal color measurement

The color changes of the first floret were measured using a portable colorimeter (CHROMA METER CR-400, KONICA MINOLTA, INC, JAPAN). Calibration (L* = 91.73, a* = -0.80, b* = 4.89) was performed with a white standard plate. The color of five florets and 1 cm of dorsal petal margins (3 points in each measurement) were analyzed at each stage. Colorimetric parameters (L*, a*, b*, h°) were determined based on the CIE system. The L* values include the range from 0 to 100 and represent darkness and brightness, respectively. The a* and b* contain values of − 60 to + 60. The a* negative is for green and a* positive for red. The b* negative and positive show blue and yellow, respectively. Hue angle (h°) is expressed in values from 0 to 360 degrees (0° and 360° = red, 90° = yellow, 180° = green and 270° = blue).

Total chlorophyll and carotenoids measurement

Chlorophyll and carotenoid contents were measured at eight-time points according to the Lichtenthaler method (Lichtenthaler and Wellburn 1983; Lichtenthaler and Buschmann 2005). The absorption of pigments was determined against 100% acetone in a spectrophotometer (SP-UV 200, Spectrum Instruments Limited, Australia) at 470, 645, and 662 nm. The concentration of pigments was calculated and plotted against time points.

Starch content measurement

Starch content was determined using the McCready method (McCready et al. 1950). For extraction and measurement of starch, 80% ethanol, 52% perchloric acid, and anthrone reagent were used. The factor of 0.90 was applied to the conversion of acid hydrolysis-glucose values to starch.

Transmission electron microscopy (TEM)

The first floret and the right dorsal petal (upper lip) margin were used for each stage's ultrastructural analysis of the petal cells (epidermal and mesophyll cells). Briefly, the petals were slowly opened at the flower bud stages. The petal tissue pieces (approximately 2×2 mm^2) were sampled using a scalpel blade under a stereomicroscope (HUND WETZLAR, Helmut Hund, Germany). Then samples were placed in a primary fixative solution (3% glutaraldehyde: 4% formaldehyde in 0.1 M phosphate buffer, pH 7.2) for 2 h at 4 °C. After washing again with the same buffer three times (10 min each time) and transferring to the TEM laboratory, the samples were subsequently fixed in 1% OsO_4 solution (in 0.1 M phosphate buffer) at room temperature for 2 h in a chemical hood. After washing with 0.1 M PBS three times (10 min each time), dehydration of fixed materials was performed in graded series of ethanol, acetone, and acetone-resin mixture

(50/50). After this step, the samples were embedded in 60 °C epoxy resin for 48 h. Ultrathin (50–100 nm) cross-sections of the petal were obtained using an ultramicrotome (Leica Ultracut-R ultramicrotome, Wetzlar, Germany) and collected on standard 200 mesh copper grids. These sections were firstly stained in 20% uranyl acetate solution in pure methanol for 20 min and then in lead citrate solution (Reynolds solution) for 5 min (Reynolds 1963). TEM micrographs of epidermal and mesophyll cells were acquired using a transmission electron microscope (EM208S, PHILIPS, Nederland) at 100 kV and analyzed with ImageJ software version 1.52. We used five micrographs for the frequency of mesophyll cells (with the same plastid morphology) per stage. Also, four cells were analyzed in each micrograph.

Phenolics measurement

Methanolic extract from frozen petal tissue was prepared using the Wang procedure (Wang et al. 2015), collected in dark bottles, and used for further analysis. The total phenolic content (TPC) was quantified according to the Folin-Ciocalteu method (Singleton et al. 1965), with a minor modification. The absorbance of the samples was read at 765 nm. Gallic acid was considered as standard. TPC was expressed as µg gallic acid equivalent (GAE) per 1 g FW. Total flavonoid content (TFC) was measured using the aluminum chloride method with a minor modification (Zhishen et al. 1999). The samples absorbance was read at 510 nm. Quercetin was used as a standard. TFC was expressed as µg quercetin equivalent (QE) per 1 g FW. The pH differential method was used to calculate the total monomeric anthocyanin content (TMAC), as described by Wroistad (Wroistad 1993). The TMAC was expressed as µg cyanidin-3-glucoside equivalents (C3GE) per 1 g FW, as follows:

$$A = (A_{510} - A_{700})_{pH1} - (A_{510} - A_{700})_{pH4.5}$$

$$TMAC = \frac{(A \times MW \times DF \times V_e \times 1000)}{(\varepsilon \times 1 \times M)}$$

MW: molecular weight of cyanidin-3-glucoside (449.2 g/mol).

DF: dilution factor.

V_e: extract volume.ε: molar extinction coefficient of cyanidin-3-glucoside (26,900)

M: mass of the petals extracted.

Statistical analysis

This study followed a completely randomized design (CRD) with five replications. The experiment was repeated at least once. All quantitative data were subjected to one-way ANOVA using SAS 9.1 to indicate significant differences. Means were separated at a 5% level of probability by Duncan's Multiple Range Test. All graphs were drawn with Excel. All data were expressed on a fresh weight basis.

Result

Time-course of snapdragon (*Antirrhinum majus* 'Legend White') development and senescence

The first morphological symptom of senescence (or wilting) appeared at S6, which was accompanied by translucent petal margins. The wilting became clearer at S7 (severe wilting). Then the corolla collapsed (Fig. 1A). Fresh weight (FW) increased until S5 and then declined, confirmed by visual signs of senescence (Fig. 1B). Dry weight (DW) was decreased after S5 and continued until S8 (Fig. 1C). Ion leakage, as one of the indicators of senescence progress in petals, increased after the flower opening stage (S4) and reached the highest value at S8 (Fig. 1D). The cell sap pH increased from S1 to S3. Then it decreased from the flower opening stage (S4) to the desiccated flower stage (S8) (Fig. 1E). These results indicated that pH changes affect the color changes of the white petals.

Petal color modifications

The significant difference in the colorimetric parameters indicated that the color changes in the white petals are present (Table 2). With the progress of flower development and senescence, the lightness parameter (L*) showed a similar trend from S1 to S6. At S7, an increase in the L* parameter was observed, and then the brightness of the petals decreased. Parameter a*, as an indicator of the green–red color of the petal texture, was the highest after the full-opened flowers and the subsequent stages. The lowest value was observed at S2 and S3. Significant changes were observed in the parameter b* (blue-yellow). As expected, flower bud stages (S1, S2, and S3) were characterized by high b* values. Then, a sharp decrease in b* occurred at S5, and with the progress of senescence at the later stages, the value of b* increased. Moreover, the hue angle (0º-360º) decreased after the S5, and the lowest h^0 was recorded at S7 and S8.

Changes in the pigments and starch content

As is evident in Fig. 2, chlorophyll a, b, and carotenoid content decreased in the developing petals and reached the lowest amount at the stage of a flower opening. However, a lower amount of chlorophyll and carotenoids were measured at later stages. In this experiment, starch content showed a

Fig. 1 A Morphological changes of the petal color in eight stages of snapdragon (*Antirrhinum majus* 'Legend White') flower life from development to senescence: S1 tight green bud; S2 emerging bud; S3 full bud; S4 half-opened flower; S5 fully opened flower; S6 wilted flower; S7 collapsed flower; S8 desiccated flower. **B** Fresh weight (FW), **C** dry weight (DW), **D** ion leakage rate, and **E** the cell sap pH of snapdragon (*Antirrhinum majus* 'Legend White') petals during development and senescence. Different letters indicate significant differences determined using Duncan's multiple-range test ($p < 0.05$). Error bars represent $\pm$ SE, n = 5
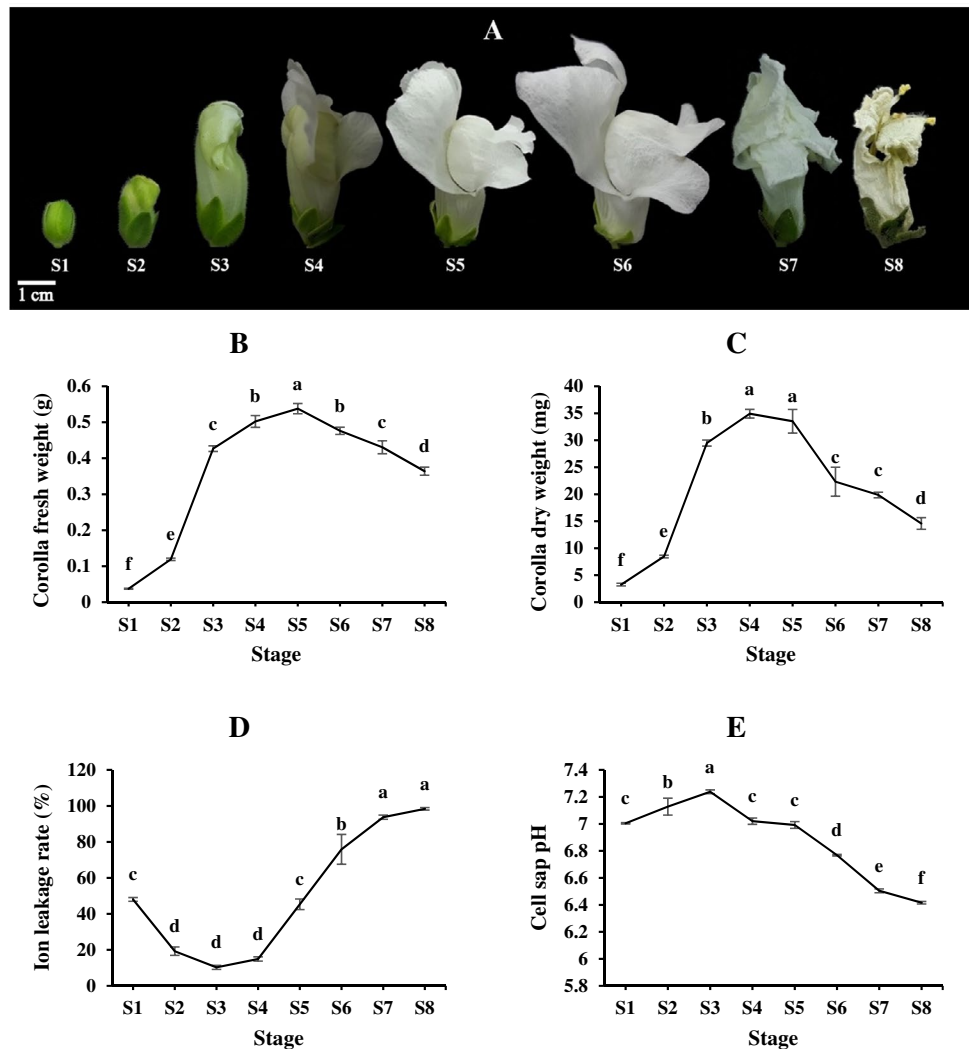
significant difference at stages of development and senescence (Fig. 2D). At S1 and S2, starch content was highest. As the flowers developed and senescence begin, starch granules were degraded, and the starch content reached to lowest value. At S8, compared with S1, starch content fell to 77%.

Plastid morphology

The Plastids morphology of petal cells (epidermis and mesophyll) in the snapdragon was examined using TEM analysis. The results of TEM observations at S1 indicated that both epidermal cells and mesophyll cells of green petals had chloroplasts that did not morphologically differ. Both cell types had clear and abundant thylakoid structures and intact envelope membranes. Moreover, evident starch granules were observed in these chloroplasts (Fig. 3A). The result indicated that 59% of the mesophyll cells have such morphology (Fig. 4G). At S2, fewer thylakoid membranes with starch granules were observed in the chloroplasts of both cell

types. In addition, thylakoid structures showed less electron density (Fig. 3B, arrows). S2 morphology was observed in 52% of mesophyll cells (Fig. 4G). The plastid morphology was dramatically altered at S3. At this stage and in some epidermal cells, starch granules disappeared, granum structures collapsed, thylakoid membranes were unclear, and several electron-dense globules (white arrows) were mainly found on the surface of thylakoid membranes (Fig. 4A). Whereas in the chloroplasts of mesophyll cells, thylakoid structures faded gradually, chloroplasts were transformed into leucoplasts under the process of plastid transition and contained only starch granules (Fig. 4B). At this stage, some leucoplasts were degraded through distinct pathways. In Fig. 4C, although the envelope membrane has been destroyed, thylakoid structures were arranged as phagophore-like structures around the starch granules and formed a complete autophagosome-like organelle. This structure lacked stroma and was located inside the vacuole. In addition, numerous small vacuoles were around the leucoplasts or in contact

Table 2 Color parameters value of snapdragon (*Antirrhinum majus* 'Legend White') at flower development and senescence stages

Stage	Colorimetric parameters			
	L*	a*	b*	h⁰
S1	76.1 ± 1.4 bc	− 9.5 ± 0.8 c	28.2 ± 2.5 b	106.8 ± 0.4 b
S2	75.4 ± 0.9 bc	− 16.7 ± 0.4 d	37.9 ± 1.8 a	113.9 ± 0.4 a
S3	76.5 ± 1.2 b	− 16.1 ± 0.4 d	36.6 ± 1.1 a	113.7 ± 0.2 a
S4	75.2 ± 1.2 bc	− 4.6 ± 0.5 b	10.2 ± 1.2 d	114.3 ± 0.4 a
S5	71.7 ± 1.3 c	− 1.4 ± 0.4 a	3.6 ± 0.7 e	110.2 ± 2.1 ab
S6	76.3 ± 1.8 bc	− 2.4 ± 0.4 a	7.6 ± 1.4 de	108.1 ± 0.9 b
S7	83.9 ± 2.3 a	− 2.7 ± 0.7 a	15.3 ± 2.4 c	100.4 ± 2.2 c
S8	76.2 ± 1 bc	− 2.1 ± 0.7 a	17.6 ± 1.1 c	97 ± 2.3 c

Colorimetric parameters (L*, a*, b*, h°) have been expressed based on the CIE system. L*: lightness (0 = dark, 100 = bright); a*: green–red (negative = green, positive = red); b*: blue-yellow (negative = blue, positive = yellow), and h^0 or hue angle (0°–360°). S1, tight green bud; S2, emerging bud; S3, full bud; S4, half-opened flower; S5, fully opened flower; S6, wilted flower; S7, collapsed flower; S8, desiccated flower. Values represent the mean ± SE. Different minor letters (a–e) show significant differences among development and senescence stages ($p \leq 0.05$)

with phagophore-like structures. Some electron-dense plastoglobules were also transferred from leucoplasts to small vacuoles. Furthermore, incomplete autophagosome-like organelles were observed in some mesophyll cells. In both autophagosome-like organelles, the starch granules appear to be broken (Fig. 4D). Starch granules may be sequestered in autophagic structures (Fig. 4E, arrow) or exist freely in the cytosol (Fig. 4E, arrowhead). Also, small starch granules were placed in small vesicle-like structures or small vacuoles and budded to the outside (white arrows). This event is a type of piecemeal chlorophagy known as the small starch granule-like structure (SSGL bodies) (Fig. 4F, lower structure). Finally, the double membrane of the autophagosome-like organelles gradually disappeared and formed a vacuole-like structure. The remaining membrane may fuse with other small vacuoles (Fig. 4F, upper structure). Also, numerous small vacuoles were observed around the degrading structures. All these events were observed in only 35% of mesophyll cells (Fig. 4G). At S4, plastids were not observed, neither in the epidermal nor mesophyll cells.

Phenolic composition

TPC values were significantly different among various stages of flower development and senescence. TP content increased gradually from the flower bud stage (2925 GAE µg g⁻¹FW) to S6 (14,575 GAE µg g⁻¹FW) and decreased with cell death (Fig. 5A). This significant difference in TPC levels showed that S6 is the best stage for harvesting snapdragon flowers for commercial and edible use.

In all stages of flower development and senescence, the content of TF varied from 805 QE µg g⁻¹FW to 6505 QE µg g⁻¹FW. The S6 contained the highest amount of TFC. The lowest amount was measured at the flower bud stage.

Fig. 2 **A** Chlorophyll a, **B** chlorophyll b, **C** carotenoids, and **D** starch content of snapdragon (*Antirrhinum majus* 'Legend White') during flower development and senescence. S1, tight green bud; S2, emerging bud; S3, full bud; S4, half-opened flower; S5, fully opened flower; S6, wilted flower; S7, collapsed flower; S8, desiccated flower. Different letters indicate significant differences determined using Duncan's multiple-range test ($p < 0.05$). Error bars represent ± SE, n = 5
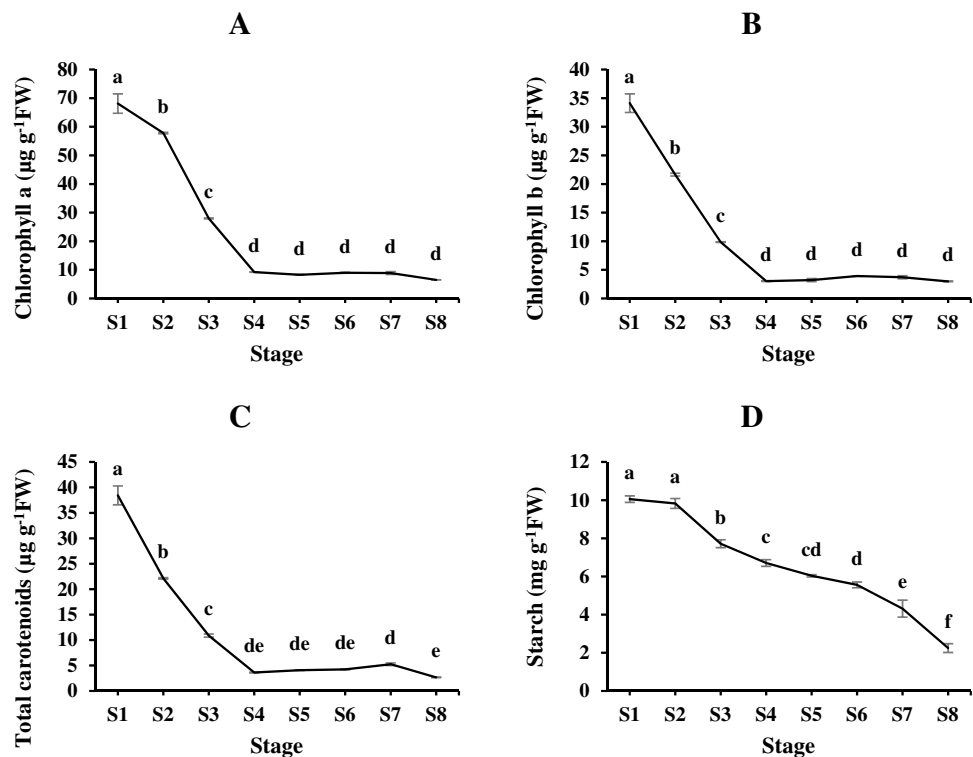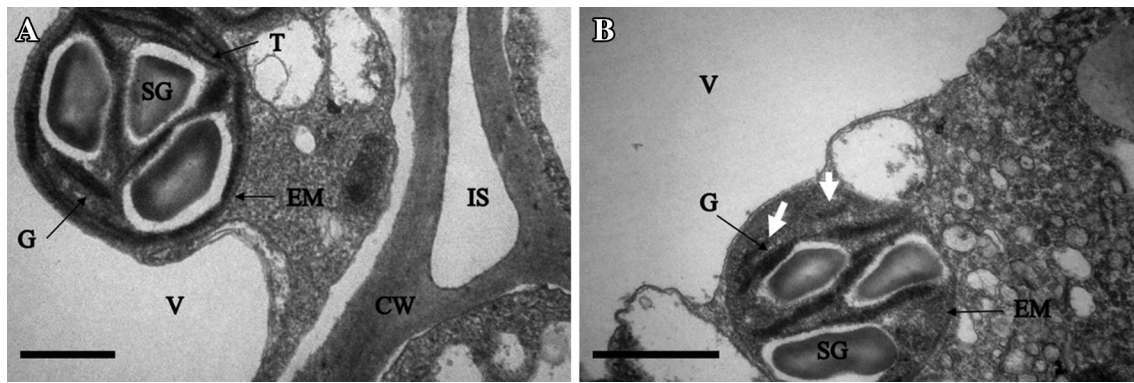
Fig. 3 Transmission electron microscopy analysis of plastids from epidermal and mesophyll cells. **A** Chloroplast of mesophyll cell, chloroplasts have clear thylakoid structures, intact envelope membranes, and evident starch granules at S1, **B** Chloroplast of the epidermal cell, chloroplasts have fewer thylakoid membranes and low electron density (white arrows) at S2. CW, cell wall; EM, envelope membrane; G, grana; IS, intercellular spaces; SG, starch granule; T, thylakoid; V, vacuole. Scale bars, 1 μm in all figures

Although anthocyanins are colored compounds inside the cells, they were measured to detect the factors affecting the color changes of white petals, and small amounts of TMAC were observed in white petals. Among all analyzed stages, TMAC showed the highest value from S3 to S7. TMAC was especially low in S1 (213.08 C3GE μg g^{-1}FW).

Discussion

One of the first well-documented events during the development and senescence of petals is change in weight (fresh and dry). In the present study, the growth of petals from the bud stage (S1) to the fully-opened flower stage (S5) coincided with the increase in FW and DW. Both indices decreased reasonably after S5 (FW falling to 32% and DW falling to 58% of highest value, respectively). Wilting of petal margins was recorded at S6, while the wilting of the entire corolla was observed three days later (S7). These changes showed that the snapdragon flower exhibits wilting and desiccation reactions during senescence and cell death. Similar trend have been reported in several studies, including *Alstroemeria* (Wagstaff et al. 2003), carnation (Li et al. 2021), and *Lilium longiflorum* (Battelli et al. 2011), and some rose cultivars (Schmitzer et al. 2010). Typically, the formation of the central vacuole, followed by water absorption, leads to the enlargement of the cells and an increase in FW (Nabipour Sanjbod et al. 2022). Decreased FW or severe wilting include tonoplast rupture, loss of turgor, increased transparency, and slow desiccation (Breeze et al. 2004). The slow dehydration and color changes caused by wilting are known as withering and are not mechanistically different (Van Doorn and Woltering 2008). These events can indicate the degradation of cellular components and remobilization processes (Breeze et al. 2004; Battelli et al. 2011).

Ion leakage occurs commonly after phospholipids degradation, plasma membrane permeability, and tonoplast rupture, which is considered a passive event. However, ion leakage may be active during senescence, resulting in the remobilization and export of ions via the phloem (Van Doorn and Woltering 2008). The result revealed that ions leaked increasingly with flower opening. This event implies that senescence and cell death begin very early in flowers, as reported in *Alstroemeria* and snapdragon senescence studies (Wagstaff et al. 2003; Nabipour Sanjbod et al. 2022). Ion leakage is affected by structural changes in cellular components. Therefore, ion leakage is an efficient senescence marker, indicating progressive PCD, and can cause de-compartmentalization of organelles and cell pH change, affecting the stability of anthocyanins, phenolic compounds, and petal color (Rehman et al. 2017).

Color changes observed during senescence are generally associated with changes in cell sap pH. Cell sap pH is frequently assimilated to the pH of the vacuole since vacuoles occupy the most cell volume (Barthe et al. 1991). The vacuolar pH of the cells is usually in the weakly acidic range, and its variations change the stability of anthocyanins and subsequently the tissue color during senescence (Schmitzer et al. 2010). The results showed that the pH of cell sap increased during development and then became more acidic during flower senescence. Low pH causes some anthocyanins not to be stable and readily hydrate and form colorless pseudo bases (Teppabut et al. 2018). Besides, it increases the activity of enzymes such as hydrolases (Phospholipases, RNases) (Barthe et al. 1991).

The green color of young petals is caused by chlorophyll in chloroplasts (Ohmiya et al. 2017). In *Arabidopsis*, the petals at the flower bud stage were all green due to the presence of chloroplasts. Then, in the later stages of flower development, the chloroplasts of the mesophyll cells converted into
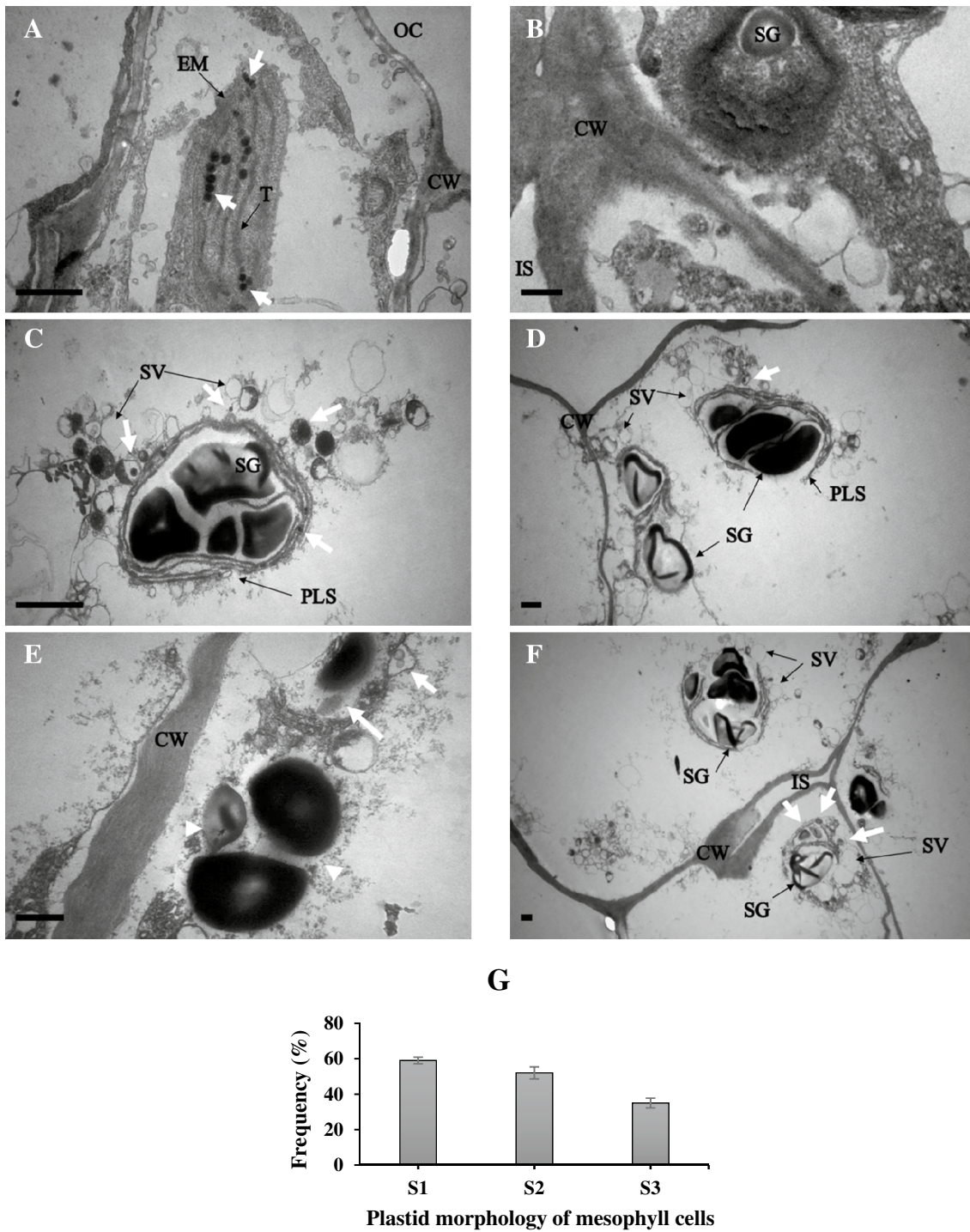
Fig. 4 Plastid morphology at full bud stage (S3), **A** Plastid of epidermal cell with unclear thylakoid membranes and electron-dense globules, **B** Leucoplast of mesophyll cell, chloroplasts were converted into leucoplasts through plastid transition, **C** Leucoplast of mesophyll cell was degraded through the formation of autophagosome-like organelle, **D** Incomplete autophagosome-like organelle with broken granule starch in mesophyll cell, **E** and **F** The occurrence of piecemeal chlorophagy in leucoplasts (**E** and lower structure in **F**) and the formation of vacuolar-like structure from autophagosomes (upper structure) in mesophyll cells. SSGL bodies have shown by white arrows, **G** Frequency of mesophyll cells with the same plastid morphology. CW, cell wall; EM, envelope membrane; G, grana; IS, intercellular spaces; OC, out of cells; PLS, phagophore-like structures; SG, starch granule; T, thylakoid; SV, small vacuole. Scale bars, 1 µm in all figures

Fig. 5 Phenolic content of snapdragon (*Antirrhinum majus* 'Legend White') during flower development and senescence. S1, tight green bud; S2, emerging bud; S3, full bud; S4, half-opened flower; S5, fully opened flower; S6, wilted flower; S7, collapsed flower; S8, desiccated flower. Different letters indicate significant differences determined using Duncan's multiple-range test ($p < 0.05$). Error bars represent ± SE, n = 5
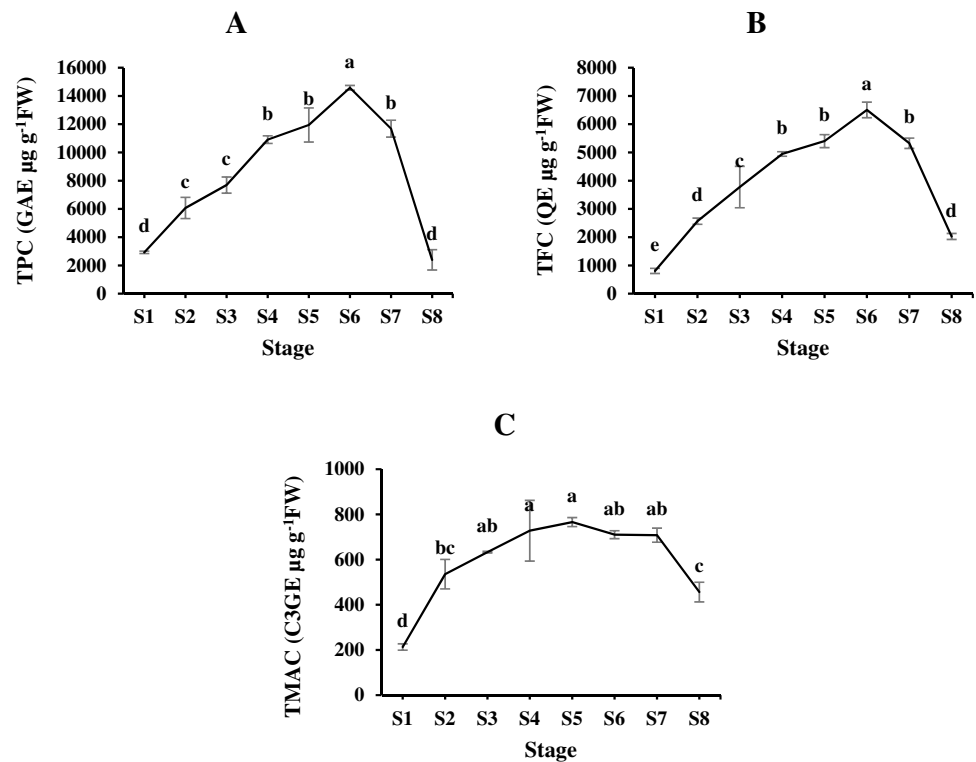
leucoplasts and disappeared (Zheng et al. 2022). Such results were also evident in the present study. At S4, there were no plastids, and the green color faded, which coincided with the increase of parameter a*. As senescence progressed and fresh and dry weight decreased, the parameter L* increased, and the petals became visually paler.

During development, carbohydrates serve as a source of energy and carbon for cell wall synthesis and cause osmotic properties, water absorption, and turgor pressure, which can lead to cell expansion and petal opening (O Donoghue 2006). Starch granules are located in plastids and are degraded accompanying plastid transition and degradation (Wang and Liu 2013; Choi et al. 2021). Our result revealed that starch degradation started before the flower opening. These events can participate in cell expansion and result in flower opening. Previous studies have elucidated the strong relationship between carbohydrate content with senescence. So, it can affect senescence-color changes (Tang et al. 2015). A decrease in starch content has been reported in species such as *Lycoris radiate* (Park et al. 2021) and *Lilium* (Zhang et al. 2021). In our study also, starch content decreased with a gentle slope during senescence. On the other hand, results have indicated that hydrolysis of starch by affecting the water potential causes wilting and color changes in *Rosa damascena* (Sood and Nagar 2003; Kanani et al. 2021a).

The TEM observations provided notable results on color changes. The chloroplasts (green) were present in both cells, but the leucoplasts (white) were only found in mesophyll cells. However, leucoplasts may be present in epidermal cells at stages other than the sampling stage. In this study, mesophyll cells underwent structural changes earlier than epidermal cells (Van Doorn and Woltering 2008; Shibuya et al. 2016). In addition, the content of carotenoids decreased with the appearance of electron-dense globules in the last stages of plastid degradation. The electron-dense globules have originated from plastoglobuli. Therefore, as the findings show, plastoglobuli can be sites for the breakdown of carotenoids (Choi et al. 2021). Transfer of electron-dense globules to small vacuoles was observed in our and Smith's results. This event probably involved lipid-protein degradation inside the vacuoles (Smith 1974; Shibuya et al. 2016). The young petals were green due to the chloroplasts with typical structures and high chlorophyll content (Zheng et al. 2022). As the flower age increased, chloroplasts of mesophyll cells converted to leucoplasts during the plastid transition (Choi et al. 2021). As a result, stroma and thylakoid structures disappeared, chlorophyll degraded, and finally, the green color faded (de-greening). Although leucoplasts were formed, they were rapidly destroyed by programmed cell death (PCD). In general, autophagy acts as the main pathway for organelles degradation, such as plastids (Zhuang and Jiang 2019; Sieńko et al. 2020). In this study, leucoplasts formed autophagosome-like organelles inside the vacuoles, which confirms the involvement of macroautophagy in leucoplasts' degradation (Otegui 2018; Zhuang and Jiang 2019). It seems that the phagophores originated from the

Table 3 Events of autophagy and phytochemical during color changes in white petals of the snapdragon (*Antirrhinum majus* 'Legend White')

Stage	Events of autophagy and phytochemical activity
S1	Natural morphology in plastids (epidermal and mesophyll cells) Increase in fresh and dry weight Increase in cell sap pH Increase in phenolic compounds
S2	Gradual degradation of thylakoids structures (epidermal and mesophyll cells) Decrease in chlorophyll content Decrease in carotenoid content Decrease in starch content
S3	The appearance of electron-dense globules (epidermal and mesophyll cells) Plastid transition (mesophyll cells) Formation of autophagosome-like organelle from leucoplasts (mesophyll cells) Piecemeal chlorophagy (mesophyll cells) Decrease in cell sap pH
S4	The disappearance of plastids (epidermal and mesophyll cells) Increase in ion leakage Increase in parameter a*
S5	Decrease in fresh and dry weight
S6	Decrease in phenolic compounds
S7	Highest of parameter L*
S8	Lowest of parameter h^0

thylakoid structures. This event is known as the whole chloroplast pathway and is reported in Izumi's study (Izumi et al. 2017). Some leucoplasts indicated another autophagy pathway called piecemeal chlorophagy. In this pathway, starch granules are placed inside vesicular structures (SSGL bodies) and delivered to vacuoles (Ishida et al. 2008; Wang and Liu 2013). These small vacuoles were fused in some places. Some autophagosome-like organelles formed structures similar to vacuoles. These events happened just before the flower opening. Studies have proven that macroautophagy and microautophagy are involved in the vacuolation process (Van Doorn et al. 2011; Nabipour Sanjbod et al. 2022). The plastids are large organelles and may participate in the formation of central vacuoles by forming autophagosomes and autophagy activity. These events could be evidence of the transformation of plastids into vacuoles.

The phenolic compounds have importance in various therapeutic, nutritional, and cosmetic aspects. Furthermore, they play a role in the color changes of petals and the production of fragrances to attract pollinators (Yáñez et al. 2012; Chamani et al. 2020). Investigation of phenolics provided information about their effective properties in the color changes of white petals and determined the best stage to extract the highest phenolic amounts. This is an effective strategy in the production of edible flowers. The results indicated that phenolic compounds were synthesized gradually by decreasing the chlorophyll and carotenoid content. Overall, the highest content of phenolics (TPC, TFC, and TMAC) was measured at the beginning stage of wilting. The increase in flavonoid content in white petals has been attributed to the synthesis of colorless compounds such as flavone,

flavonol, and flavanone (Zhao and Tao 2015). The synthesis of anthocyanins led to a decrease in the b* parameter. As senescence progressed, the content of phenolics decreased. Changes in the phenolic content during development have been reported in several species, such as Rose 'KORcrisett' (Schmitzer et al. 2009), cut H_3O rose (Chamani et al. 2020), *Helleborus niger* (Schmitzer et al. 2013), and damask rose (Kanani et al. 2021a). As senescence progressed and pH decreased, the b* parameter increased. However, the content of anthocyanins did not change. It has been shown that the decrease in pH affects the stability of anthocyanins and causes the anthocyanins to shift to colorless compounds (Teppabut et al. 2018). Mainly, the reduction of phenolic compounds in the final stages of senescence accelerates the death of petal cells under oxidative stress (Schmitzer et al. 2009). All events of autophagy and phytochemical activity are summarized in Table 3.

Conclusion

The present study investigated the background events of white petal color changes in small parts and single cells. Our emphasis for this was the effect of phytochemical compounds and autophagy pathways involved in color changes. For this purpose, a small part of the petal tissue was considered, and both epidermal cells and mesophyll cells were analyzed. The results revealed that during flower development (S1, S2, and S3), de-greening occurred, and visually the green color of the flowers faded gradually. This morphological change was associated

with some physiological processes, including a decrease in chlorophyll and carotenoid content, starch content, parameter a*, and an increase in parameter b* and color angle (h^0). In addition, the morphology of plastids changed under the plastid transition program, and chloroplasts were transformed into leucoplasts. These leucoplasts had thylakoid structures and chlorophyll in some cases. One of the astonishing findings of this study was the involvement of autophagy in leucoplasts' degradation and de-greening. Piecemeal chlorophagy was observed in starch granules degradation. Leucoplasts were also transformed into autophagosome-like organelles, which provided evidence for the transformation of plastids into vacuoles at stages before flower opening. It seems that these two autophagy processes are involved in the vacuolation process, and both cause water absorption and petal expansion. These events caused the color of the petals to change from green to yellow.

When plastids disappeared and the green color faded, the phenolic compounds were synthesized and reached the highest amount at the beginning stage of wilting. Although anthocyanins had highest values, they remained colorless because the cell sap pH decreased. Furthermore, in these stages, high amounts of flavonoids were considered due to the presence of colorless flavonoid compounds. The decrease in starch content and the subsequent decrease in water absorption caused the petal wilting and the fading of the flower color. All of these factors increased the parameter L*. Transparency of the petals was observed in the stage of severe wilting. After flower desiccation and cell death, the parameter L* and color angle decreased and was in the pale yellow range.

In addition, High levels of phenolic, after flower opening and before severe wilting, can be the best stage for harvesting snapdragon flowers for commercial and industrial use. Also, our findings provided a unique basis for studying the molecular mechanisms involved in these processes.

Data availability All data supporting the findings of the present study are available in this paper.

Declarations

Conflict of interest The authors declare that they have no conflict of interest.

References

Barthe P, Vaillant V, Gudin S (1991) pH of cell sap and vacuolar pH during senescence of the rose petal. Acta Hortic. https://doi.org/10.17660/actahortic.1991.298.14

Battelli R, Lombardi L, Rogers HJ et al (2011) Changes in ultrastructure, protease and caspase-like activities during flower senescence in *Lilium longiflorum*. Plant Sci 180:716–725. https://doi.org/10.1016/j.plantsci.2011.01.024

Breeze E, Wagstaff C, Harrison E et al (2004) Erratum: Gene expression patterns to define stages of post-harvest senescence in *Alstroemeria petals*. Plant Biotechnol J 2:155–1685. https://doi.org/10.1111/j.1467-7652.2004.00112.x

Chamani E, Wagstaff C, Kanani M (2020) Phenolics pattern of cut H3O rose flowers during floral development. Sci Hortic (amst) 271:109460. https://doi.org/10.1016/j.scienta.2020.109460

Choi H, Yi T, Ha SH (2021) Diversity of plastid types and their interconversions. Front Plant Sci 12:1–14. https://doi.org/10.3389/fpls.2021.692024

Deng C, Li S, Feng C et al (2019) Metabolite and gene expression analysis reveal the molecular mechanism for petal colour variation in six *Centaurea cyanus* cultivars. Plant Physiol Biochem 142:22–33. https://doi.org/10.1016/j.plaphy.2019.06.018

González-Barrio R, Periago MJ, Luna-Recio C et al (2018) Chemical composition of the edible flowers, pansy (*Viola wittrockiana*) and snapdragon (*Antirrhinum majus*) as new sources of bioactive compounds. Food Chem 252:373–380. https://doi.org/10.1016/j.foodchem.2018.01.102

Ishida H, Yoshimoto K, Izumi M et al (2008) Mobilization of Rubisco and stroma-localized fluorescent proteins of chloroplasts to the vacuole by an ATG gene-dependent autophagic process. Plant Physiol 148:142–155. https://doi.org/10.1104/pp.108.122770

Izumi M, Ishida H, Nakamura S, Hidema J (2017) Entire photodamaged chloroplasts are transported to the central vacuole by autophagy. Plant Cell 29:377–394. https://doi.org/10.1105/tpc.16.00637

Kanani M, Chamani E, Shokouhian AA, Torabi-Giglou M (2021a) Plant secondary metabolism and flower color changes in damask rose at different flowering development stages. Acta Physiol Plant 43:1–10. https://doi.org/10.1007/s11738-021-03200-w

Kanani M, Chamani E, Shokouhian AA, Torabi-Giglou M (2021b) Essential oil content and composition in various ecotypes of damask rose from different ecological regions. Acta Sci Pol Hortorum Cultus 20:61–69. https://doi.org/10.24326/ASPHC.2021.1.6

Li L, Yin Q, Zhang T et al (2021) Hydrogen nanobubble water delays petal senescence and prolongs the vase life of cut carnation (*Dianthus caryophyllus* L.) flowers. Plants. https://doi.org/10.3390/plants10081662

Lian Z, Huo H, Wilson SB, Chen J (2020) Development of a model mutagenesis system for snapdragon. EDIS. https://doi.org/10.32473/edis-ep584-2020

Lichtenthaler HK, Buschmann C (2005) Chlorophylls and carotenoids: measurement and characterization by UV-VIS spectroscopy. Handb Food Anal Chem 2–2:171–178. https://doi.org/10.1002/0471709085.ch21

Lichtenthaler HK, Wellburn AR (1983) Determinations of total carotenoids and chlorophylls a and b of leaf extracts in different solvents. Biochem Soc Trans 11:591–592

Liu J, Wang Y, Zhang M et al (2022) Color fading in lotus (*Nelumbo nucifera*) petals is manipulated both by anthocyanin biosynthesis reduction and active degradation. Plant Physiol Biochem 179:100–107. https://doi.org/10.1016/j.plaphy.2022.03.021

Martí-clua J (2022) Transmission electron microscopy in the study of autophagy : seeing is not always believing. Researchsquare 1–11. https://doi.org/10.21203/rs.3.rs-2271893/v1

McCready RM, Guggolz J, Silviera V, Owens HS (1950) Determination of starch and amylose in vegetables. Anal Chem 22:1156–1158. https://doi.org/10.1021/ac60045a016

Mizushima N (2022) SnapShot: organelle degradation. Mol Cell 82:1604-1604.e1

Mondal R, Antony S, Roy S, Kumar Chattopadhyay S (2022) Programmed Cell Death (PCD) in Plant: Molecular Mechanism, Regulation, and Cellular Dysfunction in Response to Development and Stress. In: Regulation and Dysfunction of Apoptosis

Nabipour Sanjbod R, Chamani E, Pourbeyrami Hir Y, Estaji A (2022) Investigation of the cell structure and organelles during autolytic PCD of *Antirrhinum majus* "Legend White" petals. Protoplasma. https://doi.org/10.1007/s00709-022-01788-5

Narbona E, del Valle JC, Arista M et al (2021) Major flower pigments originate different colour signals to pollinators. Front Ecol Evol 9:1–14. https://doi.org/10.3389/fevo.2021.743850

O Donoghue EM (2006) Flower petal cell walls: changes associated with flower opening and senescence. New Zeal J for Sci 36:130

Ohmiya A, Sasaki K, Nashima K et al (2017) Transcriptome analysis in petals and leaves of chrysanthemums with different chlorophyll levels. BMC Plant Biol 17:1–15. https://doi.org/10.1186/s12870-017-1156-6

Otegui MS (2018) Vacuolar degradation of chloroplast components: autophagy and beyond. J Exp Bot 69:741–750

Park CH, Yeo HJ, Kim YJ et al (2021) Profiles of secondary metabolites (phenolic acids, carotenoids, anthocyanins, and galantamine) and primary metabolites (carbohydrates, amino acids, and organic acids) during flower development in lycoris radiata. Biomolecules 11:1–14. https://doi.org/10.3390/biom11020248

Qi Y, Lou Q, Li H et al (2013) Anatomical and biochemical studies of bicolored flower development in *Muscari latifolium*. Protoplasma 250:1273–1281. https://doi.org/10.1007/s00709-013-0509-8

Rabiza-Świder J, Skutnik E, Jędrzejuk A, Rochala-Wojciechowska J (2020) Nanosilver and sucrose delay the senescence of cut snapdragon flowers. Postharvest Biol Technol 165:111165. https://doi.org/10.1016/j.postharvbio.2020.111165

Rehman RNU, You Y, Yang C et al (2017) Characterization of phenolic compounds and active anthocyanin degradation in crabapple (*Malus orientalis*) flowers. Hortic Environ Biotechnol 58:324–333. https://doi.org/10.1007/s13580-017-0328-5

Reynolds ES (1963) The use of lead citrate at high pH as an electron-opaque stain in electron microscopy. J Cell Biol 17:208. https://doi.org/10.1083/jcb.17.1.208

Sadali NM, Sowden RG, Ling Q, Jarvis RP (2019) Differentiation of chromoplasts and other plastids in plants. Plant Cell Rep 38:803–818. https://doi.org/10.1007/s00299-019-02420-2

Schmitzer V, Veberic R, Osterc G, Stampar F (2009) Changes in the phenolic concentration during flower development of rose "KORcrisett." J Am Soc Hortic Sci 134:491–496. https://doi.org/10.21273/jashs.134.5.491

Schmitzer V, Veberic R, Osterc G, Stampar F (2010) Color and phenolic content changes during flower development in ground-cover rose. J Am Soc Hortic Sci 135:195–202. https://doi.org/10.21273/jashs.135.3.195

Schmitzer V, Mikulic-Petkovsek M, Stampar F (2013) Sepal phenolic profile during helleborus niger flower development. J Plant Physiol 170:1407–1415. https://doi.org/10.1016/j.jplph.2013.05.012

Shibuya K, Yamada T, Ichimura K (2016) Morphological changes in senescing petal cells and the regulatory mechanism of petal senescence. J Exp Bot 67:5909–5918. https://doi.org/10.1093/jxb/erw337

Sieńko K, Poormassalehgoo A, Yamada K, Goto-Yamada S (2020) Microautophagy in plants: consideration of its molecular mechanism. Cells 9:887. https://doi.org/10.3390/cells9040887

Singleton VL, Rossi JA Jr (1965) Colorimetry of total phenolics with phosphomolybdic-phosphotungstic acid reagents. Am J Enol Vitic 16:144–158

Smith CG (1974) The ultrastructural development of spherosomes and oil bodies in the developing embryo of *Crambe abyssinica*. Planta 119:125–142. https://doi.org/10.1007/BF00390886

Sood S, Nagar PK (2003) Changes in abscisic acid and phenols during flower development in two diverse species of rose. Acta Physiol Plant 25:411–416. https://doi.org/10.1007/s11738-003-0023-2

Sun X, Qin M, Yu Q et al (2021) Molecular understanding of postharvest flower opening and senescence. Mol Hortic 1:1–12. https://doi.org/10.1186/s43897-021-00015-8

Tang G, Li X, Lin L et al (2015) Combined effects of girdling and leaf removal on fluorescence characteristic of *Alhagi sparsifolia* leaf senescence. Plant Biol 17:980–989. https://doi.org/10.1111/plb.12309

Teppabut Y, Oyama KI, Kondo T, Yoshida K (2018) Change of petals' color and chemical components in *Oenothera* flowers during senescence. Molecules. https://doi.org/10.3390/molecules23071698

Van Doorn WG, Woltering EJ (2008) Physiology and molecular biology of petal senescence. J Exp Bot 59:453–480. https://doi.org/10.1093/jxb/erm356

Van Doorn WG, Kirasak K, Sonong A et al (2011) Do plastids in *Dendrobium* cv. Lucky Duan petals function similar to autophagosomes and autolysosomes? Autophagy 7:584–597. https://doi.org/10.4161/auto.7.6.15099

Van Doorn WG, Kirasak K, Ketsa S (2015) Macroautophagy and microautophagy in relation to vacuole formation in mesophyll cells of *Dendrobium* tepals. J Plant Physiol 177:67–73. https://doi.org/10.1016/j.jplph.2015.01.006

Wagstaff C, Malcolm P, Rafiq A et al (2003) Programmed cell death (PCD) processes begin extremely early in Alstroemeria petal senescence. New Phytol 160:49–59. https://doi.org/10.1046/j.1469-8137.2003.00853.x

Wang Y, Liu Y (2013) Autophagic degradation of leaf starch in plants. Autophagy 9:1247–1248. https://doi.org/10.4161/auto.25176

Wang X, Li C, Liang D et al (2015) Phenolic compounds and antioxidant activity in red-fleshed apples. J Funct Foods 18:1086–1094. https://doi.org/10.1016/j.jff.2014.06.013

Woltering EJ, Van Doorn WG (1988) Role of ethylene in senescence of petals—morphological and taxonomical relationships. J Exp Bot 39:1605–1616. https://doi.org/10.1093/jxb/39.11.1605

Wroistad RE (1993) Color and pigment analyses in fruit products. Agric Exp Stn, pp 4–20

Yáñez JA, Remsberg CM, Takemoto JK et al (2012) Polyphenols and flavonoids: an overview. In: Roufogalis B (ed) Flavonoid pharmacokinetics: methods of analysis, preclinical and clinical pharmacokinetics, safety, and toxicology. Wiley, Hoboken, pp 1–69

Yeon JY, Kim WS (2020) Positive correlation between color and scent in rose petals with floral bud development. Hortic Sci Technol 38:608–619. https://doi.org/10.7235/HORT.20200056

Zhang Y, Zhong D, Liu Z, Gao J (2021) Study on the physiological, cellular, and morphological aspects of the postharvest development of cut lily flowers. Hortic Plant J 7:149–158. https://doi.org/10.1016/j.hpj.2021.02.005

Zhao D, Tao J (2015) Recent advances on the development and regulation of flower color in ornamental plants. Front Plant Sci 6:261. https://doi.org/10.3389/fpls.2015.00261

Zhao L, Xia Y, Wu X-YY et al (2018) Phenotypic analysis and molecular markers of leaf senescence. Methods Mol Biol 1744:35–48. https://doi.org/10.1007/978-1-4939-7672-0_3

Zheng X, Lan J, Yu H et al (2022) Arabidopsis transcription factor TCP4 represses chlorophyll biosynthesis to prevent petal greening. Plant Commun. https://doi.org/10.1016/j.xplc.2022.100309

Zhishen J, Mengcheng T, Jianming W (1999) The determination of flavonoid contents in mulberry and their scavenging effects on superoxide radicals. Food Chem 64:555–559. https://doi.org/10.1016/S0308-8146(98)00102-2

Zhuang X, Jiang L (2019) Chloroplast degradation: multiple routes into the vacuole. Front Plant Sci 10:1–8